

**Statistica Sinica Preprint No: SS- 2021-0147**

<b>Title</b>	Robust Shape Matrix Estimation for High-Dimensional Compositional Data with Application to Microbial Inter-Taxa Analysis
<b>Manuscript ID</b>	SS-2021-0147
<b>URL</b>	<a href="http://www.stat.sinica.edu.tw/statistica/">http://www.stat.sinica.edu.tw/statistica/</a>
<b>DOI</b>	10.5705/ss.202021.0147
<b>Complete List of Authors</b>	Danning Li, Arun Srinivasan, Lingzhou Xue and Xiang Zhan
<b>Corresponding Authors</b>	Lingzhou Xue Xiang Zhan
<b>E-mails</b>	lzxue@psu.edu zhanx@bjmu.edu.cn

# Robust Shape Matrix Estimation for High-Dimensional Compositional Data with Application to Microbial Inter-Taxa Analysis

Danning Li<sup>1</sup>, Arun Srinivasan<sup>2</sup>, Lingzhou Xue<sup>2</sup> and Xiang Zhan<sup>3</sup>

<sup>1</sup>*KLAS and School of Mathematics & Statistics, Northeast Normal University*

<sup>2</sup>*Department of Statistics, Pennsylvania State University*

<sup>3</sup>*Department of Biostatistics, School of Public Health and BICMR, Peking University*

*Abstract:*

Estimating the dependence structure in the data is a key task when analyzing compositional data. Real-world compositional data sets are often complex owing to high-dimensionality, heavy tails, and the possible existence of outliers. We consider a general class of elliptical distributions to model the heavy-tailed distribution of latent log-basis variables, which is characterized by a latent shape matrix. The latent shape matrix is a scalar multiple of the latent covariance matrix, when it exists, and it can preserve the directional properties of the dependence in a distribution when the covariance matrix does not exist. We propose using a robust composition-adjusted thresholding procedure based on Tyler's M-estimator to estimate the latent shape matrices of high-dimensional compositional data from different groups. We prove appealing theoretical properties under the high-dimensional setting. Simulation studies and a real application to microbial inter-taxa analysis demonstrate the numerical properties of the proposed method.

---

*Key words and phrases:* Elliptical distribution, Compositional data; Human microbiome research, Shape matrix, Thresholding, Tyler's M Estimation.

## 1. Introduction

Compositional data arise naturally in many research topics in biology, ecology, finance, geology, and other areas. For example, compositional data are used to assess the relative proportions of chemicals within stones across different geographical locations in geology (Thomas and Aitchison, 2005), and to analyze relative market share while dynamically accounting for the total market size in economics (Arata and Onozaki, 2017). This study is motivated by inter-taxa analyses of microbiome compositional data in the rapidly growing field of human microbiome research (Cho and Blaser, 2012). It is known that an accurate estimation of the dependence structure between bacteria leads to a better understanding of the underlying mechanisms of disease development (Friedman and Alm, 2012; Goodrich et al., 2014). We focus on estimating the dependence structure of high-dimensional compositional data, which is a fundamental problem in microbial inter-taxa analysis.

Sparse estimations of large covariance or correlation matrices study the dependence structure under the assumption that only a small proportion of variables are correlated with one another. See Bickel and Levina (2008), Rothman

---

et al. (2009), Cai and Liu (2011), Bien and Tibshirani (2011), Cai et al. (2012), Rothman (2012), Xue et al. (2012), Xue and Zou (2014a), Fan et al. (2016), Bien (2019), among others, for related papers in this topic. However, it is nontrivial to estimate the sparse covariance matrix of high-dimensional compositional data, the data matrix of which induces a sum-to-one constraint for each row and is intrinsically not full rank. The compositional data analysis framework proposed by Aitchison (1986) lays the bedrock for the study of the dependency structure of compositional data. Under this latent framework, the sparse correlations for compositional data (sparCC) method proposed by Friedman and Alm (2012) employs an iterative algorithm to estimate the correlation matrix. The sparCC method does not guarantee that the estimator is positive-definite or that correlations are bounded between  $[-1, 1]$ . To solve these issues, Fang et al. (2015) developed the correlation inference for compositional data through Lasso (CCLasso) method, which employs an  $\ell_1$ -penalization to estimate a sparse representation of the latent correlation matrix and ensure the positive definiteness. Recently, Cao et al. (2019) introduced the composition-adjusted thresholding (COAT) procedure for estimating the sparse covariance matrix of compositional data under a latent data framework.

Existing covariance or correlation estimation procedures for compositional data, including the aforementioned sparCC, CCLasso, and COAT, are essentially

---

built on regularized sample covariance matrices. They all assume sub-Gaussian tails or even normal distributions for the latent log-basis variables (Cao et al., 2019). However, it is known that the sample covariance matrix behaves poorly when the data deviate significantly from normality (Tyler, 1987; Nordhausen and Tyler, 2015). Owing to machine error, natural variation, or experimental procedure, real-world compositional data sets are riddled with outliers and heavy tails.

Another key rationale for developing our method is to create a method that fits naturally into a practical data analysis pipeline. While classic estimation of a single dependency structure is common, researchers often wish to compare across multiple cohorts simultaneously (Morgan et al., 2015). This motivates a joint analysis viewpoint, because the estimation of multiple dependence structures provides additional insights when studying compositions across multiple groups. For example, one may be interested in learning how the dependence of a microbiome changes in the presence or absence of antibiotics regimes, or between disease cohorts. However, across cohorts, there may be key dependencies that remain the same, regardless of the clinical covariate. Therefore, a joint estimation is useful, because it shares information across groups in order to improve accuracy.

Our primary contribution is the development of the HeavyCOAT procedure,

---

which provides an accurate joint estimation of the orientation and spread of the underlying elliptical contours, even when the covariance matrix may not exist. We focus on estimating the dependence structure from the shape matrix in a wide class of elliptical distributions. We propose a robust composition-adjusted thresholding procedure, called HeavyCOAT, to estimate the sparse latent shape matrix of high-dimensional compositional data under the general elliptical distribution framework. The HeavyCOAT procedure first estimates the shape matrix of the transformed data  $\mathbb{X}_c$  across each cohort of interest, and then uses the estimated shape matrices to construct a sparse estimation of the latent shape matrices of each row of  $\mathbb{Y}$  for each cohort by solving a positive-definite thresholding problem. By using either a fused or a group penalty (Tibshirani et al., 2005; Friedman et al., 2010; Danaher et al., 2014) in the positive-definite thresholding step, the HeavyCOAT method can jointly estimate multiple sparse latent shape matrices when the observed compositions come from different groups and their shape matrices share a certain similarity.

From a theoretical viewpoint, we study the asymptotic behaviors of the proposed method. Primarily, we show that the HeavyCOAT procedure is a robust estimator that effectively recovers the sparsity pattern of the dependence structure and achieves sign consistency with high probability under the broad class of elliptical distributions. In addition, we derive the convergence rate under the

---

spectral norm for the estimation of a sparse latent shape sub-matrix as well as the explicit expected risk bound under the squared spectral norm. The derived convergence rate and risk bound are comparable with optimal results under Gaussian or sub-Gaussian tail conditions. We also demonstrate the finite-sample properties of the HeavyCOAT procedure and present a real application to microbial inter-taxa analysis.

The rest of this paper is organized as follows. After introducing a general class of elliptical distributions and notation in Section 2, we present the HeavyCOAT procedure in Section 3. Section 4 presents the asymptotic properties, including the selection consistency, sign consistency, convergence rate, and risk bound. We evaluate the finite-sample properties using simulation studies in Section 5, and present a real application to microbial inter-taxa analysis in Section 6. Section 7 concludes the paper. Technical proofs and additional simulations are presented in the online Supplementary Material.

## **2. Preliminaries**

### **2.1 Problem Setting**

The challenges of compositional data analysis arise from the transformation of unconstrained features to the compositional space (Aitchison, 1986). We first introduce the notation under the single-group setting and the latent view of compo-

## 2.1 Problem Setting

sitional data analysis popularized by Cao et al. (2019). Let  $\mathbf{W}_0 \in \mathbb{R}_+^{p_0}$  be a vector of basis variables and  $\mathbf{Y}_0 = \log(\mathbf{W}_0)$  be a vector of latent log-basis variables. The corresponding compositional random vector  $\mathbf{X}_{0,i} = (X_{0,i,1}, \dots, X_{0,i,p_0})'$  is generated by normalizing  $X_{0,i} = W_{0,i} / \sum_{i=1}^{p_0} W_{0,i}$ . In practice, we often observe only the compositional data matrix  $\mathbb{X}_0 = (\mathbf{X}_{0,1}, \dots, \mathbf{X}_{0,n})'$ . Instead of the basis matrix  $\mathbb{W}_0 = (\mathbf{W}_{0,1}, \dots, \mathbf{W}_{0,n})'$ , where  $n$  denotes the number of observations. For example, in microbiome research, raw DNA totals vary greatly between samples, and thus the relative proportions  $\mathbb{X}_0$  are reported (Li, 2015). To account for the compositional structure of  $\mathbb{X}_0$ , the centered log-ratio (clr) transformation is used as a preprocessing step on  $\mathbb{X}_0$ . Specifically, we have  $\mathbb{X}_c = \text{clr}(\mathbb{X}_0) = (\log(X_{0,i,j}/g(\mathbf{X}_{0,i})))$ , for  $i = 1, \dots, n$  and  $j = 1, \dots, p_0$ , where  $g(\mathbf{X}_{0,i})$  is the geometric mean of  $\mathbf{X}_{0,i} = (X_{0,i,1}, \dots, X_{0,i,p_0})'$ . The goal of this study is to use the observations  $\mathbf{X}_{0,i}$ , where  $i = 1, \dots, n$ , to make an inference on the dependence structure of  $\mathbf{Y}_0 = (\mathbf{Y}_{0,1}, \dots, \mathbf{Y}_{0,n})'$ , where  $i = 1, \dots, n$ , which is the true dependence relationship we wish to capture.

To allow for heavy tails and possible outliers, we assume that each  $\mathbf{Y}_{0,i} \in \mathbb{R}^{p_0}$  follows an elliptical distribution such that  $\mathbf{Y}_{0,i} \sim \mathcal{E}_{p_0}(\mu, \Sigma_0, \phi)$ , where  $\mathcal{E}_{p_0}(\mu, \Sigma_0, \phi)$  is a  $p_0$ -dimensional elliptical distribution with the location parameter  $\mu \in \mathbb{R}^{p_0}$ , positive-definite shape matrix  $\Sigma_0$ , and density generator  $\phi$  (Cambanis et al., 1981; Tyler, 1987; Fang et al., 1990). By Cambanis et al. (1981),

## 2.1 Problem Setting

---

$\mathbf{Y}_{0,i}$  is equivalently represented as

$$\mathbf{Y}_{0,i} = \mu + u_i(\Sigma_0)^{1/2}\xi_i,$$

where  $\xi_i$  is drawn uniformly from  $\mathbb{S}^{p_0-1}$ , and  $u_i$  is an arbitrary random variable or deterministic nonzero scalar, independent of  $\xi_i$ . Note that  $\mathcal{E}_{p_0}(\mu, \Sigma_0, \phi)$  consists of a large class of distributions with elliptically shaped contours, including the Gaussian distribution and heavy-tailed distributions such as the Laplace and Cauchy distributions, which are often used to generate data efficiently from the elliptical distribution (Andrews and Mallows, 1974; Goes et al., 2020; Müller and Richter, 2019). Let  $u_i$  be a scalar random variable, and  $\xi_i \sim \mathcal{N}(\mathbf{0}, \mathbf{I}_{p_0 \times p_0})$ . The Gaussian scale mixture random variable  $\mathbf{Y}_{0,i} = \mu + u_i(\Sigma_0)^{1/2}\xi_i$  is a useful elliptical distribution (Goes et al., 2020). For ease of representation, we refer to these distributions according the form of  $u_i$ , for instance,  $\mathbf{Y}_{0,i}$  follows a Laplace scale mixture distribution when  $u_i$  is generated from a Laplace distribution. The underlying dependence structure is characterized by the shape matrix. If the covariance matrix exists, the shape matrix is proportional to the covariance matrix. When the covariance matrix does not exist (e.g. the Cauchy distribution), the shape matrix is still a reliable measure of directional dependence (Tyler, 1987; Nordhausen and Tyler, 2015).

## 2.2 Real-Data Motivation

As a practical illustration of this problem setting, we use the mucosal membrane data set collected by Morgan et al. (2015) to illustrate the non-normality and heavy-tails in the microbiome compositional data. We conduct several normality tests (e.g., the Cramer–von Mises test (Cramér, 1928), Lilliefors test (Conover, 1998), and Shapiro–Francia test (Shapiro and Francia, 1972)) to check whether each column of  $Y_0$  is normally distributed with an  $\alpha$ -level threshold 0.05 or with the Bonferroni-adjusted  $\alpha$ -level threshold. The results of these tests are summarized in Table 1. Across all normality tests, most of the taxa fail to satisfy the assumed normal distribution, suggesting the presence of non-normal behavior.

Table 1: Number of rejections of three different tests of normality among the 200 most abundant taxa. Each test is evaluated at a threshold of 0.05 and the Bonferroni-adjusted threshold.

Test of normality for each taxa		
Method	Threshold	Number of Rejections
Cramer-von Mises	.05	200
	.05/200	197
Lilliefors	.05	199
	.05/200	198
Shapiro-Francia	.05	199
	.05/200	198

### 2.3 The Shape Matrix

To study the dependence structure of compositional data, we consider a general class of elliptical distributions characterized by the shape matrix (Cambanis et al., 1981; Fang et al., 1990). It is known that the shape matrix is a scalar multiple of the covariance matrix, when it exists, and that it can preserve the directional properties of the dependence in a distribution, without requiring the existence of moments (Tyler, 1987; Nordhausen and Tyler, 2015; Wiesel and Zhang, 2015). This is particularly useful in microbiome analysis, because the shape matrix allows us to recover the linear relationship between microbial taxa, even in extremely noisy practical data settings. In such settings, the error within the data may not fit the classical Gaussian assumption. For example, if the  $(i, j)$  element of the shape matrix is positive, then taxa  $i$  is positively and linearly associated with taxa  $j$ . Therefore, as the abundance of taxa  $i$  increases, the abundance of taxa  $j$  increases. If the  $(i, j)$  element of the shape matrix is zero, then there is no association between the abundances of taxa  $i$  and taxa  $j$ .

In view of these appealing properties, the shape matrix can be viewed as a promising alternative to the covariance matrix for heavy-tailed distributions. The shape matrix can be estimated efficiently even when the second moment is not bounded (Tyler, 1987). We use a simulation study to explore the interpretation of the shape matrix and also the impact of heavy tails. In this toy example, we gen-

### 2.3 The Shape Matrix

---

erate  $n = 500$  independent bivariate realizations from a Gaussian scale mixture distribution. We provide more insight into scale mixture distributions in Section 2. We consider three different choices of  $u_i$ : the multivariate normal distribution with  $\{u_i\}_{i=1}^n = 1$ , the Laplace scale mixture with  $u_i \sim \text{Laplace}(0, 1)$ , and the Cauchy scale mixture with  $u_i \sim \text{Cauchy}(0, 1/100)$ . The diagonal elements of the shape matrix are fixed as one and we vary the off-diagonal dependence strength  $C \in \{-.5, 0, .5\}$ . In the first two settings, the covariance matrix exists and  $C$  coincides with the correlation.

We compare four measures of bivariate dependence in this simulation study: the Pearson correlation coefficient (denoted by  $P$ ), Kendall correlation coefficient (denoted by  $K$ ), Spearman correlation coefficient (denoted by  $S$ ), and normalized Tyler's M-estimator (Tyler, 1987) of the shape matrix (denoted by  $T$ ). As shown in Table 2, all four measures perform well in the Gaussian setting. Tyler's M-estimation and rank correlations can capture the underlying dependence under all three settings, while the Pearson correlation coefficient performs poorly in both the Laplace and the Cauchy settings, owing to heavy-tails. Overall, Tyler's M-estimation provides a more accurate estimation than both the rank correlations and the Pearson correlation estimates, which motivates us to propose new methods for the robust estimation of the shape matrix  $\Sigma_0$  of the latent variables  $\mathbb{Y}_0$ .

Table 2: Illustration of the shape matrix measuring dependence. The estimated correlation is listed for a given true correlation  $C$  under each scale mixture.

Method	Gaussian			Laplace			Cauchy		
$C$	-0.5	0	0.5	-0.5	0	0.5	-0.5	0	0.5
$T$	-0.48	0.04	0.42	-0.44	-0.01	0.51	-0.50	0.08	0.48
$K$	-0.34	0.02	0.30	-0.30	0.00	0.37	-0.37	0.03	0.33
$S$	-0.49	0.04	0.44	-0.39	0.00	0.50	-0.48	0.02	0.42
$P$	-0.50	0.03	0.45	-0.38	0.03	0.35	-0.89	-0.95	0.93

### 3. Methodology

This section proposes a robust positive-definite estimation of sparse shape matrices for compositional data. The observed compositions may come from different cohorts, and their shape matrices may share some similarity. Suppose that there are  $K$  independent compositional data sets  $\mathbb{X}_{0,k} = (\mathbf{X}_{0,k,1}, \dots, \mathbf{X}_{0,k,n_k})' \in \mathbb{R}^{n_k \times p_0}$ , for  $k = 1, 2, \dots, K$ , and  $\mathbb{Y}_{0,k} = (\mathbf{Y}_{0,k,1}, \dots, \mathbf{Y}_{0,k,n_k})' \in \mathbb{R}^{n_k \times p_0}$  are the corresponding latent log-basis variables. For any  $p < p_0$ , the proposed method estimates the  $p \times p$  sub-matrix of the true shape matrix of  $\mathbb{Y}_{0,k}$ . The estimation of a sub-matrix is not overly restrictive because, in practice it is typical to screen out taxa with low counts or low accuracy prior to running an analysis. Furthermore, when  $p = p_0 - 1$ , this is analogous to dropping the reference components with a dependency structure that is not of interest to the researcher. We employ this in the microbial inter-taxa analysis of Section 6, where we drop the column of the OTU matrix that refers to the counts of *unclassified* microbes. Because this OTU encompasses all taxa that were not matched to known taxa of interest,

---

the dependency captured by this OTU is likely uninformative in understanding the underlying biological mechanism, and we still recover the vast majority of dependencies between taxa.

Let  $\mathbb{X}_{k,c} = (\mathbf{X}_{k,c,1}, \dots, \mathbf{X}_{k,c,n_k})' \in \mathbb{R}^{n_k \times p}$  be the sub-matrix of transformed data  $\text{clr}(\mathbb{X}_{0,k})$ , and the columns of  $\text{clr}(\mathbb{X}_{0,k})$  associated with this sub-matrix be enumerated in the index set  $\mathcal{C} \subset \{1, \dots, p_0\}$ . Without loss of generality, we assume that  $\mathcal{C} = \{1, \dots, p\}$  (i.e., we drop the  $p_0^{\text{th}}$  component). Let  $A_0 = \mathbf{I}_{p_0 \times p_0} - (1/p_0)\mathbf{1}_{p_0}\mathbf{1}_{p_0}^T$  and  $A = (\mathbf{I}_{p \times p}, \mathbf{0}_{p \times (p_0-p)}) - (1/p_0)\mathbf{1}_p\mathbf{1}_{p_0}^T$ . Lemma 1 is the key to our analysis showing how elliptical distributions are retained through transformation.

**Lemma 1.** *Suppose each  $\mathbf{Y}_{0,k,i} \in \mathbb{R}^{p_0}$  in  $\mathbb{Y}_{0,k}$  follows the elliptical distribution  $\mathcal{E}_{p_0}(\mu_k, \Sigma_{0,k}, \phi_k)$ , where  $\text{rank}(\Sigma_{0,k}) = p_0$ . Then, each  $\text{clr}(\mathbf{X}_{0,k,i})$  in  $\text{clr}(\mathbb{X}_{0,k})$  follows the elliptical distribution  $\mathcal{E}_{p_0-1}(A_0\mu_k, A_0\Sigma_{0,k}A_0^T, \phi_k)$ , and each  $\mathbf{X}_{k,c,i}$  in  $\mathbb{X}_{k,c}$  follows the elliptical distribution  $\mathcal{E}_p(A\mu_k, A\Sigma_{0,k}A^T, \phi_k)$ . Moreover, we have  $\text{rank}(A_0\Sigma_{0,k}A_0^T) = p_0 - 1$ .*

As shown in Lemma 1, the distributions of both  $\mathbf{X}_{0,k,i}$  and  $\text{clr}(\mathbf{X}_{0,k,i})$  fall in the class of elliptical distributions. In addition,  $\text{rank}(A_0\Sigma_{0,k}A_0^T) = p_0 - 1$  and  $\text{rank}(A\Sigma_{0,k}A^T) = p$ . While the shape matrix of  $\text{clr}(\mathbb{X}_{0,k})$ , that is,  $A_0\Sigma_{0,k}A_0^T \in \mathbb{R}^{p_0 \times p_0}$ , is degenerate, after removing columns relating to unimportant taxa, the shape sub-matrix of  $\mathbf{X}_{k,c,i}$ , that is,  $A\Sigma_{0,k}A^T \in \mathbb{R}^{p \times p}$ , is nondegenerate. For

---

ease of terminology, we refer to  $A\Sigma_{0,k}A^T$  as a "shape sub-matrix," which is a sub-matrix of the true shape matrix  $\Sigma_{0,k}$ . By Proposition 1 of Cao et al. (2019), the shape sub-matrix is asymptotically indistinguishable from  $\Sigma_{0,k}$  when  $\Sigma_{0,k}$  belongs to the class of sparse shape matrices explored in Section 4. Under this condition, the sparsity  $A\Sigma_{0,k}A^T$  is asymptotically equivalent to the sparsity pattern of  $\Sigma_{0,k}$ , thus allowing the shape sub-matrix to function as a proxy for the latent log-basis  $\Sigma_{0,k}$ . This asymptotic indistinguishability supports the recovery and convergence properties explored in Section 4.

Recall that the shape matrix characterizes the linear relationships between variables under the elliptical distribution framework in Section 2. Let  $\Sigma_{0,k}$  be the sparse shape sub-matrix for those latent log-basis variables  $\mathbb{Y}_{0,k}$  in the  $k$ th group. Let  $\Gamma_k$  be the corresponding shape sub-matrix for the transformed variables in  $\mathbb{X}_{k,c}$ . While  $\Sigma_{0,k}$  and  $\Gamma_k$  appear to be different estimation targets, as shown in Proposition 1 of Cao et al. (2019), the shape sub-matrix is asymptotically indistinguishable from the true log-basis shape sub-matrix, under a weak set of conditions. This relationship is a key fact that motivates the theoretical recovery properties we explore in Section 4. Under the elliptical distribution framework, we propose the HeavyCOAT procedure to first compute a robust estimation of the shape sub-matrix  $\Gamma_k$  of the transformed variables in  $\mathbb{X}_{k,c}$  (see Subsection 3.1), and then obtain a sparse estimation of the latent shape sub-matrix of the

### 3.1 Estimation Step

log-basis variables in  $\mathbb{Y}_{0,k}$  (see Subsection 3.2).

The HeavyCOAT procedure first uses Tyler's M-estimation method (Tyler, 1987) to construct a robust shape sub-matrix estimator  $\hat{\Gamma}_k$  based on the transformed data matrix  $\mathbb{X}_{k,c}$ , and then obtains the final positive-definite and sparse shape sub-matrix estimator  $\hat{\Sigma}_k$  using a subsequent joint thresholding step. Because the shape matrix is scale invariant, we may assume that  $\text{tr}(\Gamma_k) = p$ , without loss of generality (Tyler, 1987; Goes et al., 2020). Note that, under the  $K = 1$  setting, we drop the  $k$ -subscript, and the sparse estimator  $\hat{\Sigma}$ , constructed using  $\mathbb{X}_c$  as a proxy of the latent  $\mathbb{Y}_0$ , enjoys desirable theoretical properties, including selection consistency and sign consistency, which are presented in Section 4.

### 3.1 Estimation Step

For the  $k$ th group, to construct the robust shape sub-matrix estimator  $\hat{\Gamma}_k$  of the observed data matrix  $\mathbb{X}_{k,c}$ , we follow Tyler (1987) to solve the constrained optimization problem over the space of all positive-definite matrices satisfying  $\text{tr}(\Gamma_k) = p$ , that is,

$$\min_{\Gamma_k: \text{tr}(\Gamma_k)=p} \frac{p}{n_k} \sum_{i=1}^{n_k} \log((\mathbf{X}_{k,c,i})^T \Gamma_k^{-1} \mathbf{X}_{k,c,i}) + \log(\det(\Gamma_k)). \quad (3.1)$$

Optimization problem (3.1) does not require that of the covariance matrix exists, and is also agnostic to the exact functional form of the elliptical distributions,

### 3.1 Estimation Step

rather than a specific member of the class (Tyler, 1987). Hence, it can be applied to estimate the shape sub-matrix in a wide class of elliptical distributions. Although (3.1) is not a convex problem, the objective function enjoys geodesic convexity (Duembgen and Tyler, 2016).

Sun et al. (2015) and Goes et al. (2020) introduced an iterative algorithm to solve the high-dimensional Tyler's M-estimation problem. Specifically, starting from  $\tilde{\Gamma}_k^{(1)} = \alpha_k / (1 + \alpha_k) \cdot \mathbf{I}_{p \times p}$  with  $\alpha_k > \max(0, p/n_k - 1)$ , for  $t = 1, 2, \dots$ , we solve

$$\tilde{\Gamma}_k^{(t+1)} = \frac{1}{1 + \alpha_k} \frac{p}{n_k} \sum_{i=1}^{n_k} \frac{\mathbf{X}_{k,c,i} (\mathbf{X}_{k,c,i})^T}{(\mathbf{X}_{k,c,i})^T (\tilde{\Gamma}_k^{(t)})^{-1} \mathbf{X}_{k,c,i}} + \frac{\alpha_k}{1 + \alpha_k} \mathbf{I}_{p \times p}. \quad (3.2)$$

At each iteration, the diagonal element of the current estimate is increased by  $\alpha_k$  to ensure the positive definiteness, where the accuracy of the estimator is robust to the choice of  $\alpha_k$ . It is known that the iterative algorithm attains a unique solution when  $\alpha_k > \max(0, p/n_k - 1)$  (Pascal et al., 2013; Goes et al., 2020), and  $\alpha_k$  primarily controls the speed at which the algorithm converges. Thus, we can define the iterated solution for the  $k$ th group as  $\tilde{\Gamma}_k$ , and its normalization,  $\hat{\Gamma}_k$ , according to the trace constraint as

$$\hat{\Gamma}_k = \frac{p(\tilde{\Gamma}_k - \frac{\alpha_k}{1+\alpha_k} \mathbf{I}_{p \times p})}{\text{tr}(\tilde{\Gamma}_k - \frac{\alpha_k}{1+\alpha_k} \mathbf{I}_{p \times p})}. \quad (3.3)$$

Proposition 18 of Sun et al. (2014) shows that the trace normalized solution converges to the desired global minimum.

### 3.2 Thresholding Step

After obtaining the robust estimator  $\hat{\Gamma}_k$  for each class of interest, we use a positive-definite thresholding step (Rothman, 2012; Xue et al., 2012; Bien, 2019) to derive the sparse shape sub-matrix estimator  $\hat{\Sigma}_k$  of the latent log-basis variable  $\mathbb{Y}_{0,k}$  for each class by solving the following objective:

$$\hat{\Sigma}_k = \underset{\text{each } \Sigma_k \succeq \varepsilon \mathbf{I}_{p \times p}}{\operatorname{argmin}} \frac{1}{2} \sum_{k=1}^K \|\Sigma_k - \hat{\Gamma}_k\|_F^2 + P(\{\Sigma_k\}), \quad (3.4)$$

where  $\|\cdot\|_F$  denotes the Frobenius norm,  $\{\Sigma_k\}$  is the set of estimated shape matrices for each group  $k = 1, 2, \dots, K$ , and  $P(\cdot)$  denotes a convex and non-smooth penalty function of interest. Here,  $\varepsilon > 0$  ensures the positive-definite constraint. In practice, it can be taken to be a sufficiently small number, and its choice does not affect the accuracy. The constrained optimization problem (3.4) is convex and can be solved efficiently using an alternating direction method of multipliers (ADMM), presented in Section A1 of the Supplementary Material.

When  $K = 1$  and there is no cohort information to be shared, we can use the  $\ell_1$ -penalty to penalize the off-diagonal elements of  $\hat{\Sigma}$  to yield a sparse estimate. For ease of notation, we drop the subscript  $k$  in this special case when estimating  $\hat{\Sigma}$  and  $\hat{\Gamma}$ . Specifically, we use  $P(\hat{\Sigma}) = \lambda \|\hat{\Sigma}\|_{1,\text{off}}$ , where  $\lambda > 0$  is a tuning parameter and  $\|\cdot\|_{1,\text{off}}$  denotes the entry-wise  $\ell_1$ -norm of the off-diagonal elements of  $\hat{\Sigma}$ . We present theoretical results, including the selection consistency,

### 3.2 Thresholding Step

sign consistency, convergence rate, and risk bound, for this setting in Section 4.

When  $K > 1$ , we use a specific choice of  $P(\cdot)$  to borrow strength across different groups and to encourage similarity across their estimates. Two commonly used penalty functions are the *fused lasso* (Tibshirani et al., 2005) and the *group lasso* (Yuan and Lin, 2006; Friedman et al., 2010), which are useful when we are interested in learning the differential dependence structures across groups. The fused penalty

$$P(\{\Sigma_k\}) = \lambda_1 \sum_{k=1}^K \sum_{i \neq j} |\sigma_{k,ij}| + \lambda_2 \sum_{k < l} \sum_{i \neq j} |\sigma_{k,ij} - \sigma_{l,ij}|$$

encourages sparsity of the resulting covariance estimates  $\hat{\Sigma}_k$  and sparsity of their differences, where  $\lambda_1 > 0$  and  $\lambda_2 > 0$  are both tuning parameters and  $\sigma_{k,ij}$  denotes the  $(i, j)$ -element of  $\Sigma_k$ . The fused penalty encourages shared entry-wise values across different covariance estimates. On the other hand, the group penalty

$$P(\{\Sigma_k\}) = \lambda_1 \sum_{k=1}^K \sum_{i \neq j} |\sigma_{k,ij}| + \lambda_2 \sum_{i \neq j} \sqrt{\sum_{k=1}^K \sigma_{k,ij}^2}$$

uses the similarity between groups and encourages sparsity on both individual and grouped levels, where  $\lambda_1 > 0$  and  $\lambda_2 > 0$  are both tuning parameters. While the sparsity pattern of each  $\hat{\Sigma}_k$  is likely to be similar, the group penalty may be desirable when there is a shared sparsity pattern across different covariance estimates. We explore the effectiveness of these penalty functions using simu-

---

lation studies in Section 5 and a real application in Section 6. We summarize the HeavyCOAT procedure as Algorithm 1. Refer to Section A1 of the Supplementary Material for details on the algorithm and an implementation of the thresholding step.

---

**Algorithm 1** The Proposed HeavyCOAT Procedure.

**Step 1.** For  $k = 1, \dots, K$ , obtain  $\text{clr}(\mathbb{X}_{0,k})$  using the centered log-ratio transformation.

**Step 2.** For  $k = 1, \dots, K$ , construct the sub-matrix  $\mathbb{X}_{k,c}$  by selecting the columns of  $\text{clr}(\mathbb{X}_{0,k})$  enumerated in  $\mathcal{C}$ .

**Step 3.** Estimation step. For  $k = 1, \dots, K$ , solve (3.1) using (3.2) iteratively to obtain

$$\hat{\Gamma}_k = \frac{p(\tilde{\Gamma}_k - \frac{\alpha}{1+\alpha} \mathbf{I}_{p \times p})}{\text{tr}(\tilde{\Gamma}_k - \frac{\alpha}{1+\alpha} \mathbf{I}_{p \times p})}.$$

**Step 4.** Thresholding step. Obtain the sparse estimator  $\hat{\Sigma}_k$ , for  $k = 1, \dots, K$ , by solving (3.4) with the  $\ell_1$  penalty, fused penalty, or group penalty using the ADMM that is presented in Section A1 of the Supplementary Material.

---

#### 4. Theoretical Properties

This section studies the theoretical properties of the HeavyCOAT procedure when  $K = 1$ . Because we focus on  $K = 1$ , we drop the  $k$  subscript for ease of notation. Assume each latent log-basis random vector  $\mathbf{Y}_{0,i} \in \mathbb{R}^{p_0}$  in  $\mathbb{Y}_0$  follows an elliptical distribution  $\mathcal{E}_{p_0}(\mu, \Sigma_0, \phi)$ . We consider the following

---

parameter space for the sparse latent shape matrix  $\Sigma_0$ :

$$U(q, M, s_0) = \{\Sigma_0 : \Sigma_0 \succ 0, \|\Sigma_0\|_2 \leq M, \max_i \sum_{j=1}^{p_0} |\sigma_{ij}|^q \leq s_0\},$$

where  $M > 0$ ,  $q \in [0, 1)$ , and  $s_0 > 0$ . Given the above definition of  $U(q, M, s_0)$ ,

we assume

**(A1):**  $\Sigma_0 \in U(q, M, s_0)$ , with  $p_0/n \rightarrow r \in (0, +\infty)$  and  $s_0/p_0 \rightarrow 0$  as  $n \rightarrow \infty$ .

Recall that  $\hat{\Gamma}$  is a robust estimator of the shape sub-matrix  $\Gamma$  of the center log-transformed sub-matrix  $\mathbb{X}_c$ , and  $\hat{\Sigma} = (\hat{\sigma}_{ij})_{p \times p}$  is a robust estimator for of sparse latent shape sub-matrix  $\Sigma$  of the reduced set of latent log-basis variables in  $\mathbb{Y}$ . In what follows, we first study the support recovery and sign consistency in Theorems 1–2, and then explore the convergence rate under the spectral norm and the risk bound under the squared spectral norm in Theorems 3–4.

Theorems 1–2 show that the underlying shape matrix of  $\mathbb{Y}$  such as the sparsity and sign of  $\Sigma = (\sigma_{ij})_{p \times p}$ , can be estimated accurately by  $\hat{\Sigma}$  based on  $\mathbb{X}_c$ , even when the covariance matrix of  $\mathbb{Y}$  may not exist. Thus, even in extreme settings, the HeavyCOAT procedure is still able to recover the directionality of the effect.

**Theorem 1.** *Under assumption (A1), if  $\alpha > \max\{0, r - 1 + M(1 + \sqrt{r})^2\}$  and  $\lambda = C_1 \sqrt{\frac{\log(p)}{n}} + C_2 \frac{s_0}{p}$ , the sparse shape sub-matrix estimator  $\hat{\Sigma}$  satisfies*

$$P(\hat{\sigma}_{i,j} = 0 \text{ for all } (i, j) \text{ with } \sigma_{ij} = 0) \rightarrow 1, \text{ as } n \rightarrow \infty. \quad (4.5)$$

---

**Theorem 2.** Under assumption (A1), if  $\alpha > \max\{0, r - 1 + M(1 + \sqrt{r})^2\}$ ,  $\lambda = C_1 \sqrt{\frac{\log(p)}{n}} + C_2 \frac{s_0}{p}$ , and  $\lambda \leq \frac{2}{3} \min_{(i,j):\sigma_{ij} \neq 0} |\sigma_{ij}|$ , then the sparse shape sub-matrix estimator  $\hat{\Sigma}$  satisfies

$$P(\text{sgn}(\hat{\sigma}_{i,j}) = \text{sgn}(\sigma_{i,j}) \text{ for all } (i,j) \text{ with } \sigma_{i,j} \neq 0) \rightarrow 1, \text{ as } n \rightarrow \infty. \quad (4.6)$$

Theorem 3 gives the convergence rate for estimating the sparse latent shape sub-matrix  $\Sigma$  under the spectral norm.

**Theorem 3.** Under assumption (A1), if  $\alpha > \max\{0, r - 1 + M(1 + \sqrt{r})^2\}$  and  $\lambda = C_1 \sqrt{\frac{\log(p)}{n}} + C_2 \frac{s_0}{p}$ , the sparse shape sub-matrix estimator  $\hat{\Sigma}$  from (3.4) satisfies

$$\|\hat{\Sigma} - \Sigma\|_2 = O_p \left( s_0 \left( \sqrt{\frac{\log(p)}{n}} + \frac{s_0}{p} \right)^{1-q} \right). \quad (4.7)$$

The convergence rate in (4.7) is comparable with that of the COAT method (Cao et al., 2019). We consider a robust estimation under a larger class of elliptical distributions, whereas the COAT method imposes the sub-Gaussian tail condition. Similarly to COAT, (4.7) can be decomposed into an estimation error ( $\sqrt{\log(p)/n}$ ) of  $\Sigma$  and an approximation error ( $s_0/p$ ) from using the transformed data  $\mathbb{X}_c$  as a proxy for the latent log-basis variables in  $\mathbb{Y}$ . Thus, our method also shows the appealing "blessing of dimensionality" because the estimation error dominates the approximation error as  $p$  increases.

---

Given the convergence rate derived in Theorem 3, we further derive the risk bound of HeavyCOAT under the squared spectral norm in Theorem 4.

**Theorem 4.** *Under Assumption (A1), if  $\alpha > \max\{0, r - 1 + M(1 + \sqrt{r})^2\}$  and  $\lambda = C_1\sqrt{\frac{\log(p)}{n}} + C_2\frac{s_0}{p}$ , the sparse shape sub-matrix estimator  $\hat{\Sigma}$  from (3.4) satisfies*

$$\sup_{\Sigma \in U(q, s_0, M)} E \|\hat{\Sigma} - \Sigma\|_2^2 \leq C_3 s_0^2 \left( C_1 \sqrt{\frac{\log(p)}{n}} + C_2 \frac{s_0}{p} \right)^{2-2q}. \quad (4.8)$$

Theorem 4 is a new theoretical result for high-dimensional compositional data analysis. Although  $\hat{\Sigma}$  is a robust estimator under the class of elliptical distributions, the obtained risk bound matches that derived under the polynomial tails in Lemma 4 of Cai and Liu (2011).

## 5. Numerical Properties

In this section, we study the numerical effectiveness of our proposed HeavyCOAT procedure under a variety of settings. We analyze the  $K = 2$  setting to demonstrate the effectiveness of the joint estimation. An analysis of the  $K = 1$  setting can be found in the Supplementary Material. We compare HeavyCOAT with three contemporary methods. As an alternative method to Tyler's M-Estimator, we consider a rank-based covariance estimator based on Spear-

## 5.1 Performance Analysis

man's  $\rho$  and Kendall's  $\tau$  (Xue and Zou, 2012, 2014b,a; Avella-Medina et al., 2018). Thus, by substituting Tyler's M-Estimator from Section 3.1 with an associated rank-based estimator, we denote the methods as kCOAT for the Kendall's  $\tau$ -based estimator and as sCOAT for the Spearman's  $\rho$ -based estimator. Finally, we compare HeavyCOAT with the sample covariance-based COAT procedure (Cao et al., 2019). In all cases, we employ the universal thresholding procedure employed in Section 3.2 to ensure a positive-definite final estimate. If the group penalty is used, we append a -G suffix, and if the fused penalty is used, we append an -F suffix.

### 5.1 Performance Analysis

We study each method across a variety of scale mixture settings, as outlined in Section 2. That is, we study the Gaussian setting where  $u_i = 1$  for all  $i$ , the Laplace setting where  $u_i \sim \text{Laplace}(0, 1)$ , the  $T_5$  setting where  $u_i \sim t_5$ , and the extreme Cauchy setting where  $u_i \sim \text{Cauchy}(0, 1)$ . For brevity, we present the results for the heavy-tailed Laplace and  $T_5$  settings; the Gaussian and Cauchy results can be found in the Supplementary Material.

We study the following two covariance models. Let the operation  $\text{bdiag}(A, B)$  denote creating a block-diagonal matrix with diagonal blocks  $A$  and  $B$ .

1. (Sparse Covariance)  $\Sigma_{0,1} = \text{bdiag}(B_1, 4\mathbf{I}_{p_2 \times p_2})$  is a block-diagonal matrix,

## 5.1 Performance Analysis

with  $B_1 = B + \varepsilon \mathbf{I}_{p_1}$  and  $\varepsilon = \max(-\lambda_{\min}(B), 0) + .01$ , for  $p_1 = \lfloor 2\sqrt{p_0} \rfloor$  and  $p_2 = p_0 - p_1$ . The sub-matrix  $B$  is constructed to be a random symmetric matrix, with lower triangular elements drawn uniformly from  $U(-2, -4) \cup U(2, 4)$  with probability 0.15, and zero otherwise. Given  $\Sigma_{0,1}$ , we generate  $\Sigma_{0,2}$  by replacing each nonzero, nondiagonal element of  $\Sigma_{0,2}$  with zero with probability 0.7.

2. (Block Covariance) Let  $A_r$ , for  $r = 1, \dots, 10$ , be  $\frac{p_0}{10} \times \frac{p_0}{10}$  matrices, where  $A_{r,i,j} = 4(.7^{|i-j|})$  and  $B = 3I_{\frac{p_0}{10} \times \frac{p_0}{10}}$ . Construct  $\Sigma_{0,1} = \text{bdiag}(A_1, \dots, A_{10})$  and  $\Sigma_{0,2} = \text{bdiag}(A_1, \dots, A_7, B, B, B)$  as two block diagonal matrices.

The sparse covariance structure is similar to the sparse setting studied by Cai et al. (2007). The block covariance structure consists of 10 blocks that follow an AR model similar to that studied by Bickel and Levina (2008). In this case, while each block matrix may not be sparse, the magnitudes of each  $A_r$  block decay rapidly. In both cases, we construct  $\Sigma_{0,2}$  by removing nonzero elements of  $\Sigma_{0,1}$ . Thus, for the non-removed elements,  $\Sigma_{0,2}$  shares structural and magnitude information with  $\Sigma_{0,1}$ . To match the trace constraint that is assumed for the shape matrix, we normalize  $\Sigma_{0,1}$  and  $\Sigma_{0,2}$  such that  $\text{tr}(\Sigma_{0,1}) = p$  and  $\text{tr}(\Sigma_{0,2}) = p$ , as in (3.3).

We analyze the setting where  $n = 100$  and  $p_0 \in \{150, 200, 250\}$ . Given this, our estimation target is the  $p \times p$  sub-matrix, where  $p = p_0 - 1$  of  $\Sigma_{0,1}$  and  $\Sigma_{0,2}$ ,

## 5.1 Performance Analysis

denoted as  $\Sigma_1$  and  $\Sigma_2$ , respectively formed by dropping the  $p_0^{\text{th}}$  column of  $\mathbb{X}_c$ . We repeat the estimation process over  $s = 100$  replications, and assess the performance of our method by comparing the average Frobenius norm  $\frac{1}{2} \sum_{k=1}^2 \|\Sigma_k - \hat{\Sigma}_k\|_F$ , average spectral norm  $\frac{1}{2} \sum_{k=1}^2 \|\Sigma_k - \hat{\Sigma}_k\|_2$ , average true positive rate (TPR)  $\frac{1}{2} \sum_{k=1}^2 \text{TPR}_k$ , and average false positive rate (FPR)  $\frac{1}{2} \sum_{k=1}^2 \text{FPR}_k$ , where,

$$\text{TPR}_k = \frac{\#\{(i, j) : \hat{\sigma}_{k,i,j} \neq 0 \text{ and } \sigma_{k,i,j} \neq 0\}}{\#\{(i, j) : \sigma_{k,i,j} \neq 0\}}$$

$$\text{FPR}_k = \frac{\#\{(i, j) : \hat{\sigma}_{k,i,j} \neq 0 \text{ and } \sigma_{k,i,j} = 0\}}{\#\{(i, j) : \hat{\sigma}_{k,i,j} \neq 0\}}.$$

Note that  $\text{FPR}_k$  is defined to be zero if  $\#\{(i, j) : \hat{\sigma}_{k,i,j} \neq 0\} = 0$ . We select  $\lambda_1$  and  $\lambda_2$  using the cross-validation procedure outlined in Danaher et al. (2014). Following Xue et al. (2012) and Goes et al. (2020), we set  $\psi = 2$  and  $\alpha = \max(p/n - 1, 0) + 1$ . The results for the sparse covariance setting can be seen in Table 4, and the results for the block covariance setting are found in Table 5.

Across the Laplace and  $T_5$  error settings, regardless of covariance structure, the HeavyCOAT procedure performs well in terms of both norms (specifically the spectral norm) and selection consistency. Both kCOAT and sCOAT have theoretical convergence and accuracy guarantees when the fourth moment is bounded, although their effectiveness in more extreme settings is unclear

---

## 5.1 Performance Analysis

(Avella-Medina et al., 2018). This may be a key reason for the good performance of the rank-based methods in the  $T_5$  and Laplace settings. In comparison, HeavyCOAT does not require the same moment assumptions; thus, it can be applied more flexibly to situations in which the underlying distribution may not be known apriori. Furthermore, HeavyCOAT appears to be less conservative than the rank-based methods, allowing for a higher TPR across settings. While the FPR appears to be slightly inflated in comparison to kCOAT and sCOAT, this may be explained by differences in the  $\lambda_1$  and  $\lambda_2$  selected using the cross-validation procedure. To better understand the selection power of HeavyCOAT compared with that of kCOAT and sCOAT, we compare these methods under the sparse covariance setting using an ROC analysis in Section 5.2.

---

---

Table 3 and Table 4 are about here.

---

---

In both the block and sparse settings, we see an improved robust analysis over the sample covariance in the presence of heavy tails. COAT performs poorly in terms of its error compared with all robust methods, because the sample covariance suffers as the tails become heavier. Furthermore, the FPR of the COAT methods may be more than twice as large as that of HeavyCOAT, depending on the choice of penalty. This is likely due to poor estimation in the estimation step causing errors to propagate down to the thresholding step, yielding inappropriate results. Thus, when we may suspect the presence of heavy

tails, a robust viewpoint is a necessity.

## 5.2 ROC Analysis

In this section, we compare the performance of HeavyCOAT, kCOAT, and sCOAT using receiver operating characteristic (ROC) curves. This analysis, enables us to demonstrate the improved performance of our proposed HeavyCOAT procedure across various choices of the tuning parameters  $\lambda_1$  and  $\lambda_2$ . We focus on comparing the sparse covariance across the Gaussian, Laplace, and  $T_5$  settings. We also analyze the ROC curves under both the group penalty (Figure 1) and the fused penalty (Figure 2).

These curves show that our proposed HeavyCOAT procedure dominates the competitive procedures, regardless of the error type or penalty function. The kCOAT and sCOAT procedures are similar, which matches our previous numerical results. In the Gaussian setting, all methods are relatively comparable, which is to be expected, because this setting exhibits no heavy-tailed behavior.

## 6. Application to Microbial Inter-Taxa Analysis

In this section, we illustrate the potential usefulness of our method using microbiome data collected from  $n = 255$  patients that exhibit forms of gastrointestinal disease (Morgan et al., 2015). For these individuals, various experimental factors

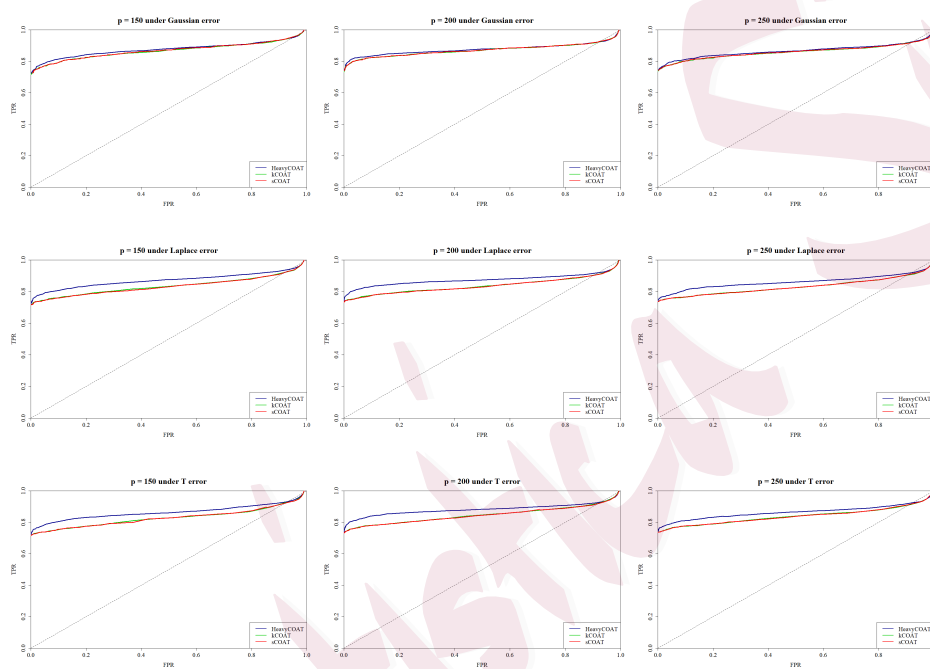


Figure 1: ROC curves for the choice of  $\lambda_1$  and  $\lambda_2$  for the sparse covariance setting under the group lasso penalty. We compare HeavyCOAT, kCOAT, and sCOAT across the Gaussian, Laplace, and  $T_5$  scale mixture models.

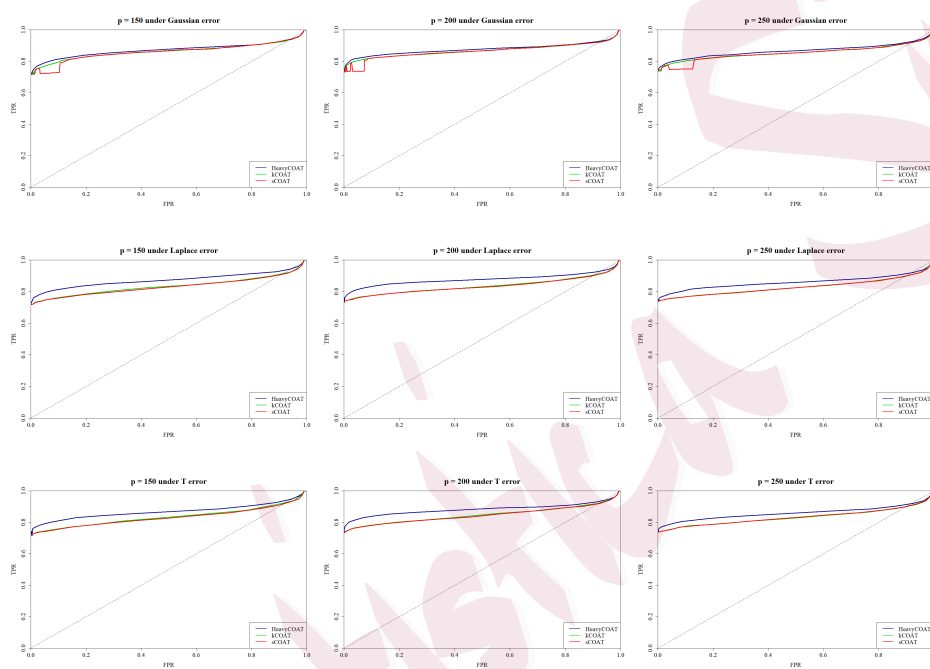


Figure 2: ROC curves for the choice of  $\lambda_1$  and  $\lambda_2$  for the sparse covariance setting under the fused lasso penalty. We compare HeavyCOAT, kCOAT, and sCOAT across the Gaussian, Laplace, and  $T_5$  scale mixture models.

---

were recorded, including the use of antibiotics and the specific type of disease. The use of antibiotics has been well studied and greatly reduces microbiome diversity in patients (Morgan et al., 2015; Dudek-Wicher et al., 2018). with regard to disease type, pouchitis refers to the inflammation of the ileal pouch which may become a chronic condition that often requires surgical intervention. The composition of the microbiome has been linked to the development of pouchitis. However, individuals with familial adenomatous polyposis (FAP) undergo a similar surgical intervention to that of individuals with inflammatory bowel disease, though often do not develop pouchitis. Thus, because pouchitis is influenced by the microbial composition, it is of interest to study the microbial dependence relationships of FAP patients to elucidate any differences. For the disease-type analyses, the patients are split into two groups: FAP and non-FAP. In both the antibiotics and the disease type analysis, it is of particular interest to study the relationships between these bacterial taxa, because inter-taxa dependence is linked to various risk factors (Morgan et al., 2015; Becker et al., 2015).

In these data, the microbial community was measured using 16s rRNA sequencing, and sequence counts were clustered as operational taxonomic units (OTU), representing biological taxa (Morgan et al., 2015). In particular, the target microbiome data set consists of 7000 species-level OTUs, which have been further classified into  $p_0 = 303$  genera to reduce sequencing errors (Li, 2015).

---

We focus on the sub-matrix of  $p = 302$  genera by omitting the category of *unclassified* taxa. Of the 255 patients,  $n_1 = 66$  had used antibiotics in the previous month before sampling, and  $n_2 = 189$  did not take antibiotics.

The patients were also classified by disease type, where  $n_1 = 39$  patients were classified with FAP, and  $n_2 = 216$  were classified as non-FAP. In these two-class cases, the choice of penalty function should be motivated by the underlying biological framework. It is known that antibiotics are extremely influential and can greatly alter the microbiome composition (Morgan et al., 2015; Dudek-Wicher et al., 2018). It is likely that the microbes that survive after an antibiotics regimen retain similar dependence relationships, but it is unlikely that the antibiotics group and the non-antibiotics group share similar values between their underlying shape matrices. Thus, we use the group lasso penalty to encourage the shared sparsity pattern, and borrow information less aggressively. On the other hand, as noted by Morgan et al. (2015), the difference in the microbiome composition between disease type is not a major factor. It is reasonable to assume that the dependence structures and strengths between both disease-type groups are similar. Employing the fused penalty in this setting is desirable, because it improves the estimation by strongly leveraging information on both the sparsity structure and the covariance magnitude.

The correlation matrices are constructed by applying HeavyCOAT with the

---

group penalty for the antibiotics and non-antibiotics groups, and applying the fused penalty for the disease-type analysis. To visualize these interactions, we represent the correlation matrices using network graphs. To ensure network stability, we implement a bootstrapping procedure to capture the relevant edges. For each setting, we construct networks from applying our HeavyCOAT procedure across 50 bootstrapped samples. We retain the edges that appear in at least 95% of the bootstrapped replicates, thereby presenting the most stable interactions within the microbial network. The thickness of an edge represents the strength of the correlation between the nodes. The results for the antibiotics setting can be found in Figure 3 and those for the disease setting can be found in Figure 4. To better understand the structure of these networks, we further implement the Louvain method for community detection (Blondel et al., 2008) to identify sub-communities of taxa within the correlation networks. These communities are denoted by the circular or square node shapes in Figure 3 and Figure 4. In all settings, we identify two unique clustering of taxa. Finally, we compute key network statistics (average correlation and average node degree) for each setting in Table 3.

For ease of presentation, we present the relationships between the top 40 genera of these phyla, because they are likely to be the most influential. We color each node by the corresponding phyla. With the effect of antibiotics in

---

Table 3: Average network statistics across group settings. The Degree column denotes the average degree across all nodes within the network, and the Correlation column lists the average correlation coefficient between taxa within each network.

Setting	Degree	Correlation
Antibiotics	7.10	0.162
No Antibiotics	16.27	0.158
FAP	11.36	0.193
non-FAP	11.36	0.200

Figure 3, we observed a marked change in the sparsity pattern, as expected. First, after antibiotic use, the overall diversity of the microbial network is drastically reduced, with far fewer active edges, which can be seen by the large reduction in the average degree in the antibiotic setting. This reduction in microbial diversity is well studied (Hildebrand et al., 2019), because there may be fundamental disruptions in these microbial systems after antibiotic use (Schwartz et al., 2020; Xu et al., 2020; Seelbinder et al., 2020). For example, we observe that genera primarily of the *Firmicutes* phylum remain active. Recent literature has shown that members of the *Firmicutes* phylum may opportunistically dominate other phyla in a post-antibiotics ecosystem (Ng et al., 2019).

When analyzing the key community memberships, we focus on the four taxa identified by Morgan et al. (2015) as playing a pivotal role: *Escherichia*, *Roseburia*, *Bifidobacterium*, and *Sutterella*. When no antibiotics are used, *Escherichia* is in a unique community and *Sutterella*, *Roseburia*, and *Bifidobac-*

---

*terium* are in a unique community. However, after antibiotics have been used, *Bifidobacterium* and *Escherichia* are in a separate cluster from *Roseburia*, and *Sutterella* disappears all together. This shift in community membership, influenced by the use of antibiotics, may be further evidence that antibiotics can fundamentally affect the relationships between surviving microbial taxa.

When comparing individuals with the non-FAP disease type to those of the FAP disease type, the difference between the covariance structures are less extreme. The two settings have an identical correlation structure which is to be expected, because the fused penalty aggressively ensures similar sparsity structures between groups. However, the edge weights between groups may vary. The correlation strength in the FAP group is slightly less than that of the non-FAP group, but the difference between disease types is less extreme than the effect of antibiotics, which is expected, based on the analysis conducted by Morgan et al. (2015). Community membership also remains consistent across groups, further suggesting that disease type is not as impactful in differentiating microbial communities. In both groups, the *Firmicutes* and *Bacteroidetes* phyla are the most active, which is to be expected, because these two phyla are dominant within the gut microbiome (Hildebrand et al., 2019; Morgan et al., 2015).

---

---

Figure 3 and Figure 4 are about here.

---

---

---

## 7. Conclusion

We have proposed the HeavyCOAT procedure for estimating the latent shape sub-matrix of high-dimensional compositional data across multiple groups, which is a scalar multiple of the covariance matrix, when it exists. HeavyCOAT has improved estimation accuracy than that of existing methods, because it models heavy tails using a large class of elliptical distributions. We have shown that when  $K = 1$ , HeavyCOAT has competitive theoretical properties. When the number of groups increases, as is common in practical microbiome data analysis, using of the fused and group penalties during the thresholding step allows us to leverage power across multiple groups and improve the estimation. Finally, we applied HeavyCOAT to gut microbiome data and identified biologically significant dependence patterns.

Currently, our method is agnostic to a known structure within the data. For example, in the microbiome setting, bacterial taxa can be naturally organized by a phylogenetic tree structure, and we expect similar taxa to have similar dependence relationships. Further avenues of exploration include embedding a known structure into the thresholding scheme. For example, one can apply group thresholding to vary the thresholding intensity across groups to account for this structure.

---

## REFERENCES

### Supplementary Material

In the online Supplementary Material, we describe the ADMM for solving multiple shape matrices in the thresholding step, present simulation results under additional settings, and provide detailed technical derivations for the lemmas and theorems presented in Section 2.

### Acknowledgments

We would like to thank the editor, associate editor and referees for their helpful comments and suggestions. Danning Li was partially supported by the National Natural Science Foundation of China grant 12101116. Arun Srinivasan and Lingzhou Xue were partially supported by the National Institutes of Health grants R21AI144765 and T32GM102057, and the National Science Foundation grants DMS-1811552 and DMS-1953189.

Danning Li and Arun Srinivasan contributed equally to this work. Lingzhou Xue and Xiang Zhan are co-corresponding authors.

### References

- Aitchison, J. (1986). *The Statistical Analysis of Compositional Data*. London, UK: Chapman and Hall.
- Andrews, D. F. and C. L. Mallows (1974). Scale mixtures of normal distributions. *Journal of the Royal Statistical Society: Series B (Methodological)* 36(1), 99–102.

## REFERENCES

---

- Arata, Y. and T. Onozaki (2017). A compositional data analysis of market share dynamics. Discussion papers, Research Institute of Economy, Trade and Industry (RIETI).
- Avella-Medina, M., H. S. Battey, J. Fan, and Q. Li (2018). Robust estimation of high-dimensional covariance and precision matrices. *Biometrika* 105(2), 271–284.
- Becker, C., M. F. Neurath, and S. Wirtz (2015). The intestinal microbiota in inflammatory bowel disease. *ILAR Journal* 56(2), 192–204.
- Bickel, P. J. and E. Levina (2008). Covariance regularization by thresholding. *The Annals of Statistics* 36(6), 2577 – 2604.
- Bien, J. (2019). Graph-guided banding of the covariance matrix. *Journal of the American Statistical Association* 114(526), 782–792.
- Bien, J. and R. J. Tibshirani (2011). Sparse estimation of a covariance matrix. *Biometrika* 98(4), 807–820.
- Blondel, V., J.-L. Guillaume, R. Lambiotte, and E. Lefebvre (2008). Fast unfolding of communities in large networks. *Journal of Statistical Mechanics Theory and Experiment* 2008, P10008.
- Cai, D., X. He, and J. Han (2007). Semi-supervised discriminant analysis. In *2007 IEEE 11th International Conference on Computer Vision*, pp. 1–7.
- Cai, T. and W. Liu (2011). Adaptive thresholding for sparse covariance matrix estimation. *Journal of the American Statistical Association* 106(494), 672–684.
- Cai, T. T., H. H. Zhou, et al. (2012). Optimal rates of convergence for sparse covariance matrix estimation. *The Annals of Statistics* 40(5), 2389–2420.

## REFERENCES

---

- Cambanis, S., S. Huang, and G. Simons (1981). On the theory of elliptically contoured distributions. *Journal of Multivariate Analysis* 11(3), 368–385.
- Cao, Y., W. Lin, and H. Li (2019). Large covariance estimation for compositional data via composition-adjusted thresholding. *Journal of the American Statistical Association* 114(526), 759–772.
- Cho, I. and M. J. Blaser (2012). The human microbiome: at the interface of health and disease. *Nature Reviews Genetics* 13(4), 260.
- Conover, W. J. (1998). *Practical Nonparametric Statistics, 3rd Edition*. New York; Wiley.
- Cramér, H. (1928). On the composition of elementary errors. *Scandinavian Actuarial Journal* 1928(1), 13–74.
- Danaher, P., P. Wang, and D. M. Witten (2014, Mar). The joint graphical lasso for inverse covariance estimation across multiple classes. *Journal of the Royal Statistical Society. Series B (Statistical Methodology)* 76(2), 373–397.
- Dudek-Wicher, R., A. Junka, and M. Bartoszewicz (2018). The influence of antibiotics and dietary components on gut microbiota. *Gastroenterology Review* 13(2), 85–92.
- Duembgen, L. and D. E. Tyler (2016). Geodesic convexity and regularized scatter estimators. *arXiv preprint arXiv:1607.05455*.
- Fan, J., L. Xue, and H. Zou (2016). Multitask quantile regression under the transnormal model. *Journal of the American Statistical Association* 111(516), 1726–1735.
- Fang, H., C. Huang, H. Zhao, and M. Deng (2015). Cclasso: Correlation inference for compositional data

## REFERENCES

---

- through lasso. *Bioinformatics* 31(19), 3172–3180.
- Fang, K. T., S. Kotz, and K. W. Ng (1990). *Symmetric Multivariate and Related Distributions*. Chapman and Hall/CRC.
- Friedman, J. and E. Alm (2012). Inferring correlation networks from genomic survey data. *PLoS Computational Biology* 8(9), e1002687.
- Friedman, J., T. Hastie, and R. Tibshirani (2010). A note on the group lasso and a sparse group lasso. *arXiv preprint arXiv:1001.0736*.
- Goes, J., G. Lerman, and B. Nadler (2020). Robust sparse covariance estimation by thresholding Tyler’s M-estimator. *The Annals of Statistics* 48(1), 86 – 110.
- Goodrich, J. K., J. L. Waters, A. C. Poole, J. L. Sutter, O. Koren, R. Blekhman, M. Beaumont, W. Van Treuren, R. Knight, J. T. Bell, T. D. Spector, A. G. Clark, and R. E. Ley (2014, Nov). Human genetics shape the gut microbiome. *Cell* 159(4), 789–799.
- Hildebrand, F., L. Moitinho-Silva, S. Blasche, M. T. Jahn, T. I. Gossmann, J. Huerta-Cepas, R. Hercog, M. Luetge, M. Bahram, A. Prysxlak, R. J. Alves, S. M. Waszak, A. Zhu, L. Ye, P. I. Costea, S. Aalvink, C. Belzer, S. K. Forslund, S. Sunagawa, U. Hentschel, C. Merten, K. R. Patil, V. Benes, and P. Bork (2019). Antibiotics-induced monodominance of a novel gut bacterial order. *Gut* 68(10), 1781–1790.
- Li, H. (2015). Microbiome, metagenomics, and high-dimensional compositional data analysis. *Annual Review of Statistics and Its Application* 2, 73–94.
- Morgan, X. C., B. Kabakchiev, L. Waldron, A. D. Tyler, T. L. Tickle, R. Milgrom, J. M. Stempak, D. Gev-

## REFERENCES

---

- ers, R. J. Xavier, M. S. Silverberg, et al. (2015). Associations between host gene expression, the mucosal microbiome, and clinical outcome in the pelvic pouch of patients with inflammatory bowel disease. *Genome Biology* 16(1), 67.
- Müller, K. and W.-D. Richter (2019). On p-generalized elliptical random processes. *Journal of Statistical Distributions and Applications* 6(1), 2195–5832.
- Ng, K. M., A. Aranda-Díaz, C. Tropini, M. R. Frankel, W. Van Treuren, C. T. O’Loughlin, B. D. Merrill, F. B. Yu, K. M. Pruss, R. A. Oliveira, et al. (2019). Recovery of the gut microbiota after antibiotics depends on host diet, community context, and environmental reservoirs. *Cell host & microbe* 26(5), 650–665.
- Nordhausen, K. and D. E. Tyler (2015). A cautionary note on robust covariance plug-in methods. *Biometrika* 102(3), 573–588.
- Pascal, F., Y. Chitour, and Y. Quek (2013). Generalized robust shrinkage estimator and its application to stap detection problem. *IEEE Transactions on Signal Processing* 62(21), 5640–5651.
- Rothman, A. J. (2012). Positive definite estimators of large covariance matrices. *Biometrika* 99(3), 733–740.
- Rothman, A. J., E. Levina, and J. Zhu (2009). Generalized thresholding of large covariance matrices. *Journal of the American Statistical Association* 104(485), 177–186.
- Schwartz, D., A. Langdon, and G. Dantas (2020). Understanding the impact of antibiotic perturbation on the human microbiome. *Genome Medicine* 12, 82.

## REFERENCES

---

- Seelbinder, B., J. Chen, S. Brunke, R. Vazquez-Uribe, R. Santhaman, A.-C. Meyer, F. S. de Oliveira Lino, K.-F. Chan, D. Loos, L. Imamovic, C.-C. Tsang, R. Lam, S. Sridhar, K. Kang, B. Hube, P. Woo, M. Sommer, and G. Panagiotou (2020). Antibiotics create a shift from mutualism to competition in human gut communities with a longer-lasting impact on fungi than bacteria. *Microbiome* 8, 133.
- Shapiro, S. S. and R. S. Francia (1972). An approximate analysis of variance test for normality. *Journal of the American Statistical Association* 67(337), 215–216.
- Sun, Y., P. Babu, and D. P. Palomar (2014). Regularized tyler’s scatter estimator: Existence, uniqueness, and algorithms. *IEEE Transactions on Signal Processing* 62(19), 5143–5156.
- Sun, Y., P. Babu, and D. P. Palomar (2015). Robust estimation of structured covariance matrix for heavy-tailed elliptical distributions. *IEEE Transactions on Signal Processing* 64(14), 3576–3590.
- Thomas, C. and J. Aitchison (2005). Compositional data analysis of geological variability and process: A case study. *Mathematical Geology* 37, 753–772.
- Tibshirani, R., M. Saunders, S. Rosset, J. Zhu, and K. Knight (2005). Sparsity and smoothness via the fused lasso. *Journal of the Royal Statistical Society: Series B (Statistical Methodology)* 67(1), 91–108.
- Tyler, D. E. (1987). A distribution-free  $m$ -estimator of multivariate scatter. *The Annals of Statistics* 15(1), 234–251.
- Wiesel, A. and T. Zhang (2015). Structured robust covariance estimation. *Foundations and Trends® in Signal Processing* 8(3), 127–216.
- Xu, L., A. Surathu, I. Raplee, A. Chockalingam, S. Stewart, L. Walker, L. Sacks, V. Patel, Z. Li, and

## REFERENCES

---

- R. Rouse (2020). The effect of antibiotics on the gut microbiome: a metagenomics analysis of microbial shift and gut antibiotic resistance in antibiotic treated mice. *BMC Genomics* 21, 263.
- Xue, L., S. Ma, and H. Zou (2012). Positive-definite  $\ell_1$ -penalized estimation of large covariance matrices. *Journal of the American Statistical Association* 107(500), 1480–1491.
- Xue, L. and H. Zou (2012). Regularized rank-based estimation of high-dimensional nonparanormal graphical models. *The Annals of Statistics* 40(5), 2541–2571.
- Xue, L. and H. Zou (2014a). Optimal estimation of sparse correlation matrices of semiparametric gaussian copulas. *Statistics and its Interface* 7(2), 201–209.
- Xue, L. and H. Zou (2014b). Rank-based tapering estimation of bandable correlation matrices. *Statistica Sinica* 24(1), 83–100.
- Yuan, M. and Y. Lin (2006). Model selection and estimation in regression with grouped variables. *Journal of the Royal Statistical Society: Series B (Statistical Methodology)* 68(1), 49–67.

REFERENCES

Table 4: Comparison of the estimation and selection performance under the sparse covariance setting with  $n = 100$  and  $p_0 = 150, 200,$  and  $250$  over 100 independent repetitions.

	Laplace Mixture Setting			$T_5$ Mixture Setting		
	$p_0 = 150$	$p_0 = 200$	$p_0 = 250$	$p_0 = 150$	$p_0 = 200$	$p_0 = 250$
	Frobenius Norm					
HeavyCOAT-G	10.75	13.33	15.90	10.71	13.31	15.90
kCOAT-G	8.78	10.71	12.43	8.82	10.73	12.55
sCOAT-G	8.28	10.12	11.73	8.44	10.25	12.02
COAT-G	97.43	127.18	153.96	78.03	106.70	122.63
HeavyCOAT-F	9.99	12.14	14.13	9.96	12.14	14.13
kCOAT-F	8.44	10.13	11.47	8.40	10.05	11.42
sCOAT-F	8.44	10.13	11.47	8.40	10.05	11.42
COAT-F	89.36	112.69	142.33	70.47	92.45	103.77
	Spectral Norm					
HeavyCOAT-G	2.57	2.80	3.12	2.54	2.79	3.10
kCOAT-G	2.56	2.79	3.07	2.56	2.81	3.08
sCOAT-G	2.58	2.83	3.14	2.61	2.90	3.19
COAT-G	53.84	71.43	83.09	42.72	64.42	70.08
HeavyCOAT-F	9.99	12.14	14.13	9.96	12.14	14.13
kCOAT-F	8.44	10.13	11.47	8.40	10.05	11.42
sCOAT-F	8.44	10.13	11.47	8.40	10.05	11.42
COAT-F	89.36	112.69	142.33	70.47	92.45	103.77
	True Positive Rate					
HeavyCOAT-G	0.80	0.80	0.82	0.80	0.81	0.82
kCOAT-G	0.76	0.76	0.78	0.76	0.76	0.78
sCOAT-G	0.75	0.74	0.77	0.75	0.75	0.77
COAT-G	0.80	0.80	0.82	0.80	0.80	0.82
HeavyCOAT-F	0.78	0.77	0.80	0.77	0.77	0.80
kCOAT-F	0.74	0.74	0.77	0.74	0.74	0.76
sCOAT-F	0.74	0.74	0.77	0.74	0.74	0.76
COAT-F	0.80	0.80	0.82	0.79	0.79	0.81
	False Positive Rate					
HeavyCOAT-G	0.06	0.07	0.12	0.06	0.07	0.12
kCOAT-G	0.03	0.03	0.06	0.03	0.04	0.06
sCOAT-G	0.03	0.03	0.05	0.03	0.03	0.06
COAT-G	0.27	0.27	0.29	0.27	0.27	0.29
HeavyCOAT-F	0.05	0.05	0.10	0.05	0.05	0.10
kCOAT-F	0.02	0.02	0.05	0.02	0.03	0.05
sCOAT-F	0.02	0.02	0.05	0.02	0.03	0.05
COAT-F	0.34	0.34	0.36	0.33	0.33	0.35

REFERENCES

Table 5: Comparison of the estimation and selection performance under the block covariance setting with  $n = 100$  and  $p_0 = 150, 200,$  and  $250$  over 100 independent repetitions.

	Laplace Mixture Setting			$T_5$ Mixture Setting		
	$p_0 = 150$	$p_0 = 200$	$p_0 = 250$	$p_0 = 150$	$p_0 = 200$	$p_0 = 250$
	Frobenius Norm					
HeavyCOAT-G	15.70	19.00	22.01	15.70	19.02	22.00
kCOAT-G	15.00	17.83	20.46	14.88	17.75	20.29
sCOAT-G	14.73	17.39	19.88	14.57	17.29	19.68
COAT-G	61.31	81.85	94.76	49.86	64.11	72.14
HeavyCOAT-F	15.86	18.96	21.69	15.85	18.96	21.66
kCOAT-F	15.16	17.93	20.39	15.03	17.81	20.21
sCOAT-F	14.89	17.56	19.91	14.72	17.39	19.68
COAT-F	42.73	54.68	63.72	35.10	43.51	51.44
	Spectral Norm					
HeavyCOAT-G	3.12	3.38	3.48	3.12	3.36	3.49
kCOAT-G	3.91	4.18	4.33	3.88	4.14	4.29
sCOAT-G	4.15	4.42	4.58	4.11	4.38	4.53
COAT-G	31.85	41.24	49.06	25.76	32.56	33.02
HeavyCOAT-F	3.38	3.65	3.79	3.37	3.64	3.79
kCOAT-F	4.06	4.34	4.51	4.03	4.32	4.48
sCOAT-F	4.28	4.57	4.74	4.24	4.53	4.69
COAT-F	19.05	24.61	28.46	15.35	18.45	21.81
	True Positive Rate					
HeavyCOAT-G	0.26	0.20	0.16	0.26	0.20	0.16
kCOAT-G	0.19	0.15	0.12	0.19	0.15	0.12
sCOAT-G	0.17	0.13	0.11	0.17	0.13	0.11
COAT-G	0.30	0.27	0.24	0.28	0.25	0.22
HeavyCOAT-F	0.19	0.14	0.12	0.19	0.15	0.12
kCOAT-F	0.16	0.12	0.10	0.16	0.12	0.10
sCOAT-F	0.15	0.11	0.09	0.15	0.11	0.09
COAT-F	0.19	0.16	0.13	0.17	0.14	0.12
	False Positive Rate					
HeavyCOAT-G	0.00	0.00	0.00	0.00	0.00	0.00
kCOAT-G	0.00	0.00	0.00	0.00	0.00	0.00
sCOAT-G	0.00	0.00	0.00	0.00	0.00	0.00
COAT-G	0.23	0.23	0.23	0.23	0.23	0.23
HeavyCOAT-F	0.00	0.00	0.00	0.00	0.00	0.00
kCOAT-F	0.00	0.00	0.00	0.00	0.00	0.00
sCOAT-F	0.00	0.00	0.00	0.00	0.00	0.00
COAT-F	0.21	0.21	0.21	0.18	0.19	0.19

## REFERENCES

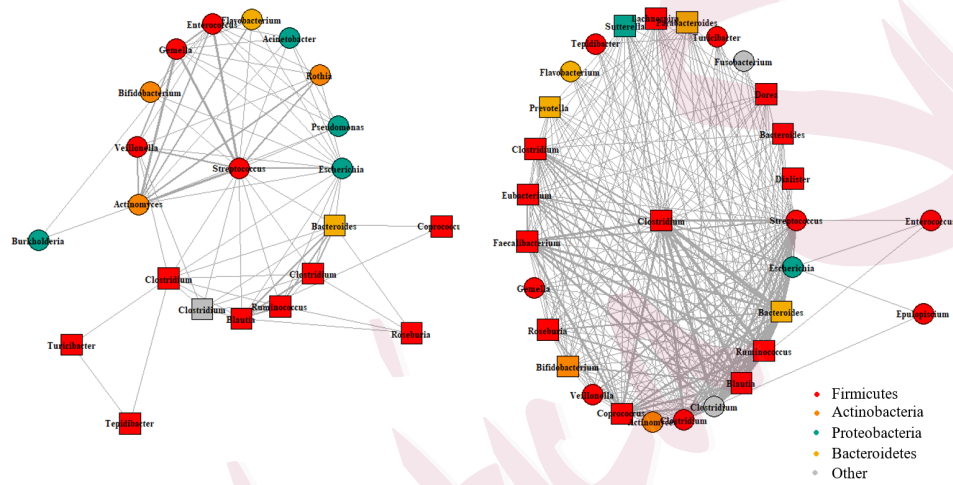


Figure 3: The estimated correlation networks between major phyla of the antibiotic group (Left) and the non-antibiotic group (Right). Taxa are sorted into communities using the Louvain method of community detection, and are identified circles and squares.

## REFERENCES

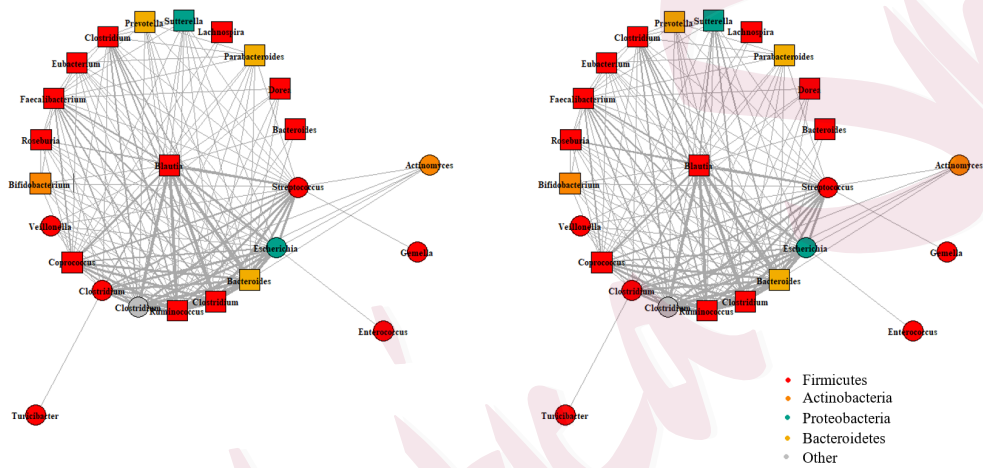


Figure 4: The estimated correlation networks between major phyla of the FAP group (Left) and the non-FAP group (Right). Taxa are sorted into communities using the Louvain method of community detection and are identified by circles and squares.

---

## REFERENCES

KLAS and School of Mathematics & Statistics, Northeast Normal University

E-mail: lidn040@nenu.edu.cn

Department of Statistics, Pennsylvania State University

E-mail: uus91@psu.edu

Department of Statistics, Pennsylvania State University

E-mail: lzxue@psu.edu

Department of Biostatistics, School of Public Health and Beijing International Center for Mathematical

Research, Peking University

E-mail: zhanx@bjmu.edu.cn